*Journal of Power Sources, 43–44* (1993) 453–460 

# Lithium/polymer/polymer solid-state rechargeable batteries

C. Arbizzani, A. M. Marinangeli, M. Mastragostino* and L. Meneghello
*Dipartimento di Chimica G. Ciamician, Università di Bologna, via Selmi 2, 40126 Bologna (Italy)*

T. Hamaide and A. Guyot
*Laboratoire des Matériaux Organiques, CNRS, BP 24, 69300 Vernaison (France)*

**Abstract**

Cycleability performance of 'tailor-made' poly(*N*-oxyalkylpyrrole) electrodes in solid-state lithium cells with poly(ethylene oxide) (PEO)-based electrolyte are compared with that of poly(N-butylpyrrole) and poly(pyrrole) electrodes. The specific effect of ether groups in improving the ionic transport in the polymer electrodes was demonstrated by determining the ion diffusion coefficients from analysis of the impedance spectra.

## Introduction

Electronically-conducting polymers are promising positive electrode materials for lithium rechargeable batteries, and lithium/polymer batteries with liquid organic electrolytes have been on the market since 1987. However, solid-state configuration is an attractive feature for consumer market batteries, and to this end, ionically-conducting polymers are promising electrolytes. Electronically-conducting polymers as well as polymer electrolytes may be easily prepared in the form of thin-layered films so that plastic-like flexible Li batteries can be manufactured.

It is, however, well known that the slowness of the ionic transport into the polymer electrodes during the electronic charge-balancing process limits the kinetics of the charge/discharge of these electrode materials, especially in solid-state cells. Indeed, while the cycleability performance of polypyrrole (pPy) is promising in Li batteries with liquid electrolyte, it is very poor in solid-state batteries with poly(ethylene oxide) (PEO)-based electrolytes [1, 2].

In order to enhance the cycleability performance of pyrrole-based polymer electrode materials in batteries with solid electrolytes, we electrosynthesized new 'tailor-made' *N*-substituted poly(pyrroles) with ether groups, starting from *N*-3-oxabutylpyrrole (NOPy), *N*-3,6-dioxaheptylpyrrole (NDPy) and *N*-3,6,9-trioxadecylpyrrole (NTPy).

Because of their known cation-coordinating properties, the ether groups were expected to improve the ionic transport into the polymer electrode. Solid-state Li batteries were assembled with these polymer electrodes and polymer electrolyte and tested by cyclic voltammetry (CV) and charge/discharge galvanostatic cycles [3–5]. In order to demonstrate the specific effect of ether groups on the kinetics of the charge/

*Author to whom correspondence should be addressed.

0378-7753/93/$6.00 

discharge process we also electrosynthesized *N*-substituted poly(pyrrole) with a butyl group starting from *N*-3-butylpyrrole (NBPy).

In the present paper we compare the cycleability performance of these *N*-substituted poly(pyrroles) to that of the pPy, both in liquid and in solid-state Li cells, and we evaluate from impedance spectra, extended over a wide frequency range, the kinetic parameters of electrochemical doping process of these polymer electrodes. Also charge/discharge data of Li/poly(*N*-oxyalkylpyrrole) batteries operating at room temperature with $(PEO–SEO)_{20}LiClO_4$ polymer electrolyte which is based on PEO and styrenic macromonomer of PEO(SEO), are reported and discussed.

## Experimental

The synthesis of the monomers NOPy, NDPy and NTPy was easily performed by the reaction of the pyrrolyl anion with the appropriate polyethyleneglycol (PEG) chloride.

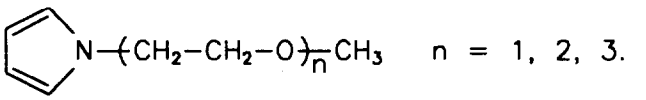


A PEG-based resin was used as solid triphase transfer-catalyst to yield *N*-alkyl product [6]. The preparation of polymer electrolyte $(PEO–SEO)_{20}LiClO_4$ is described in ref. 7. All the polymer films were galvanostatically grown on stainless-steel electrodes (surface area = 0.39 $cm^2$) at 0.8 mA $cm^{-2}$ and 25 °C by 0.17 M monomer oxidation in 0.5 M $LiClO_4$/acetonitrile (ACN) and the electrosynthesis charge was 250 mC $cm^{-2}$. In liquid cells the electrolyte was 1 M $LiClO_4$/propylene carbonate (PC); in solid cells $PEO_{20}LiClO_4$ or $(PEO–SEO)_{20}LiClO_4$ was used indifferently in the test at 70 °C as the polymer electrolyte, while at room temperature only $(PEO–SEO)_{20}LiClO_4$ was used. The Li solid-state batteries were assembled in dry box by sandwiching a Li disk (excess capacity), a thin layer of dried polymer electrolyte ($\sim 100$ $\mu$m) and a dried film of pyrrole-based polymer. Cyclic voltammetry and charge/discharge galvanostatic cycles were carried out with computer-interfaced AMEL instrumentations.

The impedance spectra of the polymer electrodes in the oxidized states were recorded over a frequency range extending from 13 mHz to 100 kHz with a Solartron frequency response analyzer (FRA model 1255) coupled to a Princeton Applied Research potentiostat (model 273). These spectra were interpreted on the basis of a modified Randles equivalent circuit shown in Fig. 1, which was developed for intercalation electrodes [8] and has been employed for polymer electrodes [9]. A nonlinear least

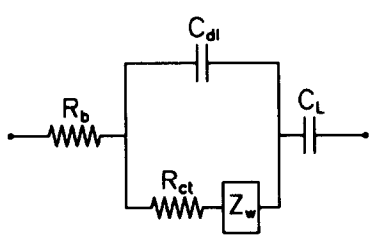


Fig. 1. Modified Randles equivalent circuit; $R_b$ = electrolyte resistance, $R_{ct}$ = charge-transfer resistance, $C_{dl}$ = double-layer capacitance, $C_L$ = limiting capacitance, $Z_w$ = Warburg impedance ($Z_w = A_w\omega^{-1/2} - jA_w\omega^{-1/2}$).

squares fitting procedure described in ref. 10 was used, and $C_{dl}$, $Z_w$ and $C_L$ were replaced by constant phase elements to account for the deviations from ideal behavior.

## Results and discussion

Figure 2 shows the CV curves at 50 mV $s^{-1}$ of the polymer electrodes in liquid at 25 °C, Fig. 2(a), and in solid-state cells at 70 °C, Fig. 2(b); the doping-level values calculated from the charge involved during the anodic wave are reported in Table 1.

In liquid electrolyte, the cycleability performance of the substituted poly(pyrroles), except pNOPy because of its very poor electronic conductivity [5], is comparable and consistent with that of pPy, given the different oxidation potentials. By contrast, in solid-state cells the cycleability performance of pNDPy and pNTPy is much better than that of pPy and pNBPy: it is almost the same in solid and in liquid cells, clearly demonstrating the specific effect of ether groups in improving cycleability.

Figure 3 shows the impedance spectra of the pNDPy electrodes in liquid, Fig. 3(a), and in solid-state, Fig. 3(b), cells, and those of pPy electrodes in both

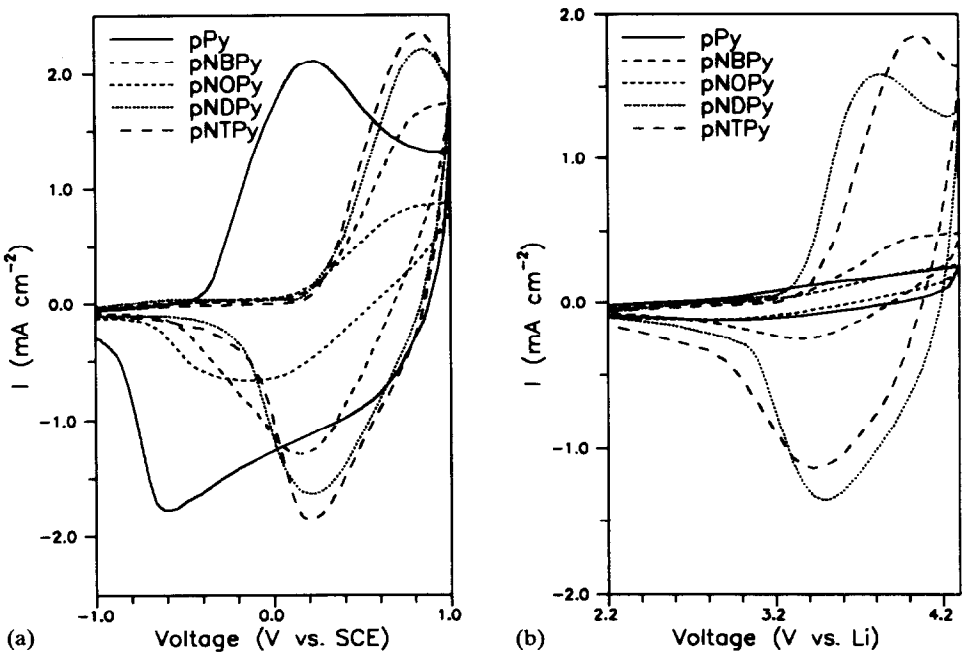


Fig. 2. Cyclic voltammogram at 50 mV $s^{-1}$ of different polymers: (a) in liquid cells at 25 °C, and (b) in solid-state cells at 70 °C.

TABLE 1

Doping level values (y%) from CVs of polymer electrodes in liquid and solid cells

| | pPy | pNBPy | pNOPy | pNDPy | pNTPy |
|---|---|---|---|---|---|
| liquid | 33 | 16 | 9 | 19 | 20 |
| solid | 4 | 7 | 3 | 23 | 18 |

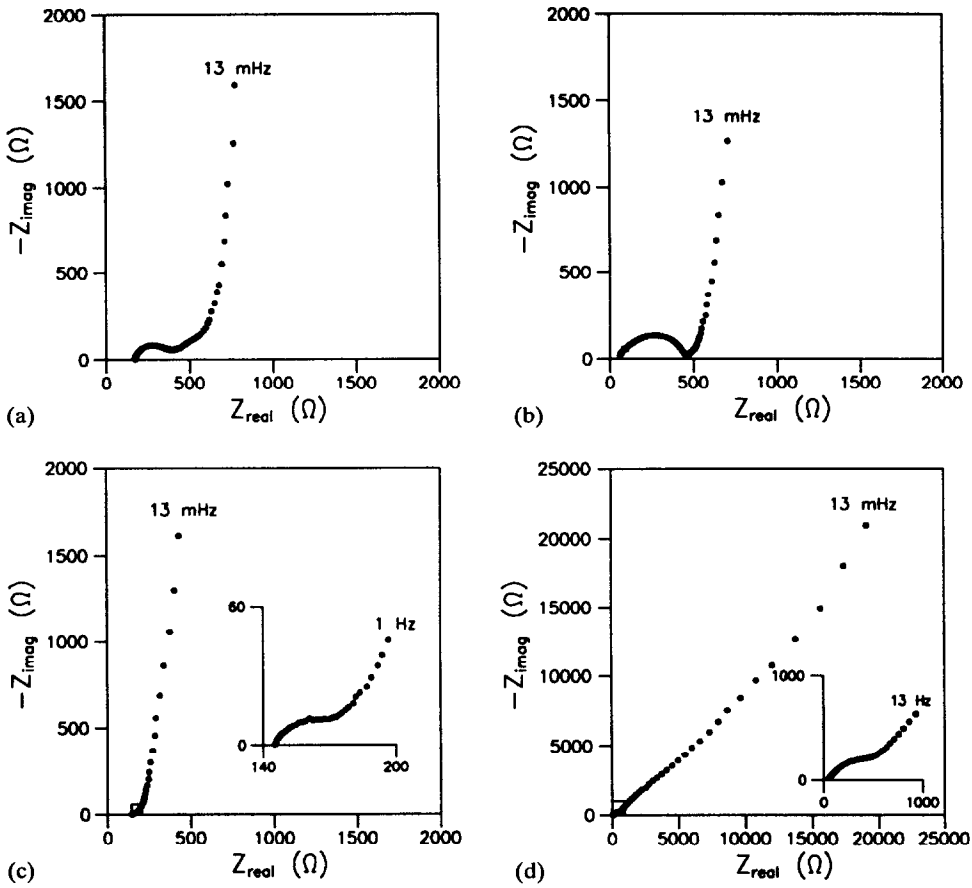


Fig. 3. FRA spectra of doped-polymer electrodes: (a) pNDPy in liquid at 25 °C; (b) pNDPy in solid-state cell at 70 °C; (c) pPy in liquid at 25 °C, and (d) pPy in solid-state cell at 70 °C.

configurations, Figs. 3(c), 3(d). The spectra of pNDPy electrodes in liquid and in solid cells are almost the same over the entire frequency region. Moreover, in the medium-frequency region (low kHz range), where the impedance response is related to charge-transfer process and displays a semicircle in the Nyquist plot, the spectrum of pPy electrode in solid cell is similar to those of pNDPy electrodes both in liquid and solid cell. By contrast, the spectrum of the pPy in liquid cell shows a semicircle with intercept on the real axis on the side of the low frequency at a lower impedance value, indicating a faster charge transfer. In the low frequency region (Hz range), where the impedance response is controlled by the diffusion of the counter ions into the polymer electrode, all the spectra display a straight line of 45° slope*. At very low frequency (mHz range) the spectra of pNDPy both in liquid and solid cells and the spectrum of pPy in liquid display a vertical line, indicating that the condition of the finite thickness has been reached. By contrast, the spectrum of pPy in solid cell show only diffusional control

*Analysis of Li/polymer electrolyte/Li cell spectra indicated that Warburg impedance in Fig. 3(b) and (d) is not due to diffusional control in the electrolyte [11].

up to ~20 kΩ real impedance value, clearly indicating that the coefficient of the counterion diffusion into the pPy, when assembled in solid-state configuration, is drastically lower than those in the other examined polymer electrodes.

In these spectra, there is good separation among the charge-transfer semicircle at high frequencies, the 45° slope of $Z_w$ at intermediate frequencies, and the vertical line at very low frequencies (except for pPy in solid cells), i.e., the phenomena associated with electrochemical process are well separated so that kinetic parameters can be evaluated. The circuit parameters determined by the fitting program are reported in Table 2, which also shows the exchange current density ($I_0$) and diffusion coefficient ($D$) values. This Table lists too the voltage to which the polymer electrodes have been potentiostatically charged up to the equilibrium and the corresponding doping levels.

The $I_0$ values were calculated from charge-transfer resistance ($R_{ct}$) data and eqn. (1), which is the linearized form of the Butler–Volmer eqn. for small overpotentials:

$$I_0 = RT/(nFAR_{ct}) \quad (1)$$

where the area $A$ is the geometrical electrode area.

The $D$ values were calculated from the limiting resistance $R_L$ values as determined from the intercept of the pseudo-capacitor straight-line to the real axis, $R_T = (R_b + R_{ct} + R_L)$, and the $C_L$ data using eqn. (2):

$$D = l^2/(3R_L C_L) \quad (2)$$

where 1 μm is taken as film thickness value. Since the relation:

$$3R_L = 2A_w^2 C_L \quad (3)$$

has to be met for the theoretical model, Table 2 also lists the parameter:

$$P = 2A_w^2 C_L/(3R_L) \quad (4)$$

to represent the consistence of our experimental data. The ion diffusion coefficient in pPy in solid-state cell can only be roughly estimated to be smaller than $3 \times 10^{-11}$ $cm^2\ s^{-1}$ because the finite thickness condition is not fully reached in the investigated frequency range.

TABLE 2

Experimental conditions, fit results of FRA of Fig. 3 and calculated $I_0$ and $D$ values

| | pNDPy in liquid | pNDPy in solid | pPy in liquid | pPy in solid |
|---|---|---|---|---|
| $E$ ( V vs. Li) | 3.7 | 3.7 | 3.3 | 3.3 |
| $y$% | 16 | 16 | 14 | 4 |
| $R_b$ (Ω) | 170 | 60 | 140 | 50 |
| $R_{ct}$ (Ω) | 180 | 400 | 30 | 400 |
| $A_w$ (Ω $s^{-1/2}$) | 240 | 120 | 120 | 5200 |
| $C_{dl}$ (μF) | 10 | 3 | 300 | 4 |
| $C_L$ (mF) | 6.7 | 7.8 | 6.2 | >6 |
| $R_T$ (Ω) | 630 | 540 | 210 | >20000 |
| $P$ | 0.92 | 0.94 | 1.5 | 5.4 |
| $I_0$ (mA $cm^{-2}$) | 0.4 | 0.2 | 2 | 0.2 |
| $D$ ($cm^2\ s^{-1}$) | $2 \times 10^{-9}$ | $5 \times 10^{-9}$ | $1 \times 10^{-8}$ | $<3 \times 10^{-11}$ |

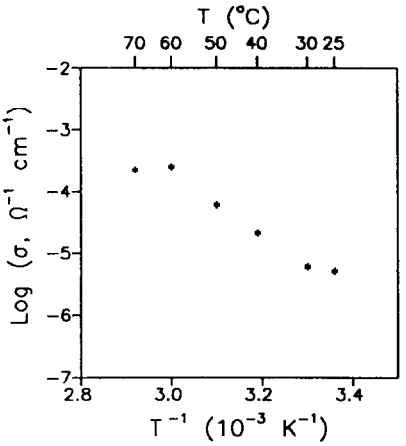


Fig. 4. Specific conductivity vs. $1/T$ of $(PEO\text{–}SEO)_{20}LiClO_4$.

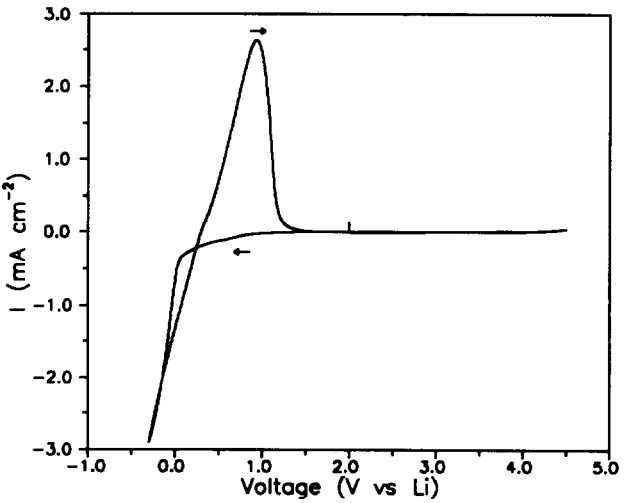


Fig. 5. Cyclic voltammogram at 50 mV $s^{-1}$ of a $(PEO\text{–}SEO)_{20}LiClO_4$ on aluminum electrode at 70 °C starting from 2 V vs. Li.

As shown in Table 2, the calculated $I_0$ value for pPy in liquid electrolyte is greater than in the other three polymer electrodes by a factor of 5 to 10. On the other hand, the $D$ value for pPy in liquid is only twice than that for pNDPy in solid state, which in turn is twice than that for pNDPy in liquid, while pPy in solid has a drastically lower $D$ value, i.e., in the order of about two or three magnitudes lower. However, by taking into account that the CVs of pPy in liquid and of pNDPy in both configurations do not indicate significant differences, clearly in all of the examined systems the $I_0$ value is not the limiting factor on the electrode performance. The poor cycleability of pPy in solid electrolyte must thus reside in the lower $D$ value only. Then, too, the fact that almost equal $D$ values were attained for pNDPy in solid and liquid electrolytes

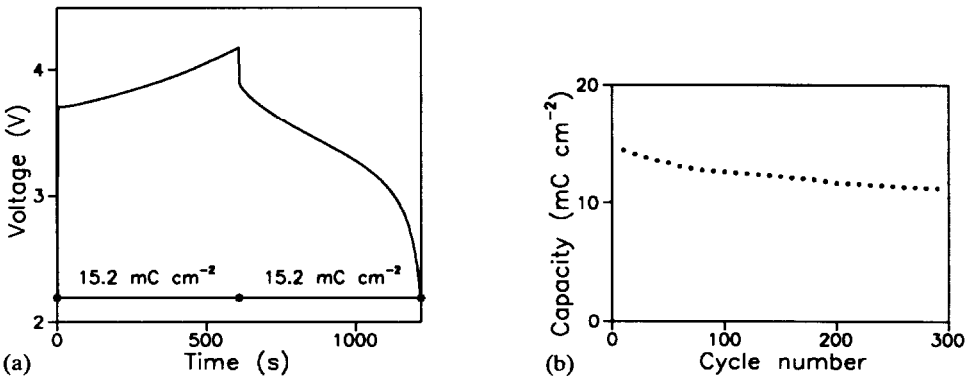


Fig. 6. (a) Galvanostatic charge/discharge cycle and (b) capacity data at different cycle number of a Li/(PEO–SEO)$_{20}$LiClO$_4$/pNTPy cell at $I=25$ $\mu$A cm$^{-2}$ and 25 °C.

is a very good result, for it demonstrates that the introduction of the ether groups enhances ionic transport in a non-swollen polymer electrode by two orders of magnitude.

Solid-state Li batteries with pNDPy and pNTPy electrodes were tested at room temperature by repeated charge/discharge galvanostatic cycles at different current densities in the potential range from 2.2 to 4.2 V using (PEO–SEO)$_{20}$LiClO$_4$ polymer electrolyte which has ionic conductivity value at 25 °C useful for practical application, as shown in Fig. 4. To characterize this polymer electrolyte, we show in Fig. 5 its CV on Al electrode, which evidences its stability over the used voltage range and the Li deposition-stripping process. Figure 6(a) shows a charge/discharge galvanostatic cycle (50th) of the battery Li/(PEO–SEO)$_{20}$LiClO$_4$/pNTPy at 25 $\mu$A cm$^{-2}$, and Fig. 6(b) the capacity data at different cycle number as evaluated by recovered charge during discharge.

## Conclusions

Our data demonstrate that substituent ether groups significantly improve the ionic transport of polypyrrole-based electrodes in solid-state configuration and that remarkable performance of solid-state Li batteries at room temperature can be achieved using (PEO–SEO)$_{20}$LiClO$_4$ polymer electrolyte. The results also evidence that discrimination among polymer electrodes is not to be done only on the basis of exchange current density values. For conducting polymers, which are a class of ion-insertion electrode materials, an important role of ionic transport in the kinetic of charge/discharge process was indeed to be expected.

## References

1 A. Corradini, M. Mastragostino, S. Panero, P. Prosperi and B. Scrosati, *Synth. Methods, 18* (1987) 625–630.
2 P. Novak and O. Inganas, *J. Electrochem. Soc., 135* (1988) 2485–2490.
3 C. Arbizzani, A. M. Marinangeli, M. Mastragostino, T. Hamaide and A. Guyot, *Synth. Methods, 41* (1991) 1147–1150.
4 M. Mastragostino, *Mater. Res. Soc. Symp. Proc., 210* (1991) 191–196.
5 C. Arbizzani, M. Mastragostino, L. Meneghello, T. Hamaide and A. Guyot, *Electrochim. Acta, 37* (1992) 1631–1634.

6 T. Hamaide, *Synth. Comm., 20* (1990) 2913–2920.
7 T. Hamaide, C. Carré and A. Guyot, *Solid State Ionics, 39* (1990) 173–186.
8 C. Ho, I. D. Raistrick and R. A. Huggins, *J. Electrochem. Soc., 127* (1980) 343–350.
9 S. Panero, P. Prosperi, S. Passerini, B. Scrosati and D. D. Perlmutter, *J. Electrochem. Soc., 136* (1989) 3729–3724.
10 B. A. Boukamp, *Solid State Ionics, 20* (1986) 31–44.
11 M. Mastragostino, unpublished data.